Applied Catalysis B: Environmental 232 (2018) 55–59

Contents lists available at ScienceDirect

Applied Catalysis B: Environmental

journal homepage: www.elsevier.com/locate/apcatb

Assessment of carbon monoxide formation in Fenton oxidation process: The critical role of pollutant nature and operating conditions

J. Carbajo*, A. Quintanilla, J.A. Casas

Chemical Engineering Section, Universidad Autonoma de Madrid, Ctra. Colmenar Km. 15, 28049 Madrid, Spain

ARTICLE INFO

Keywords:
Fenton
Advanced oxidation process
Gas phase
CO formation
CO_2 formation

ABSTRACT

This work assesses the carbon monoxide formation upon Fenton process, the most popular method for Advanced Oxidation Processes (AOPs). CO concentrations in the order of 11,000 mg/Nm^3 were measured in the Fenton oxidation of phenol after 180 min reaction at 90 °C and 3 bar. The Fenton oxidation performed on phenol and its oxidized intermediates such as hydroquinone, catechol and short-chain acids allows concluding that CO is produced through the oxidative cleavage of aromatic rings; the hydroquinone route being more selective to CO than catechol. In all cases, the carbon mass balance was satisfactorily closed to 100%. The study of the influence of the operational conditions shows that CO production is clearly favoured at H_2O_2 dosage above the stoichiometric value and low temperatures (T < 90°). The H_2O_2 dosage was the most influence variable.

The results of this work evidence for the first time the production of noxious amounts of CO along with CO_2 in Fenton processes. This finding highlights the importance of evaluating not only liquid phase intermediates due to their recalcitrant and/or toxic behavior, but also gas phase because of CO emissions.

1. Introduction

Advanced Oxidation Processes (AOPs) are efficient methods to remove pollutants in air (odour elimination, purification) [1,2], soil (remediation) [3–5] and wastewater [6–9]. AOPs are a set of processes involving the *in-situ* production of hydroxyl radicals (HO·). These radicals are one of the most powerful oxidizing agents, able to react with a wide range of organic compounds and certain inorganic pollutants (*e.g.* heavy metal or nitrates). HO· are produced by the combination of oxidant reagents (*e.g.* ozone, hydrogen peroxide, oxygen), energy sources (*e.g.* electric power, ultraviolet radiation, solar light, microwave) and/or catalysts (*e.g.* titanium dioxide, Fe salts) [10,11,12,13].

The AOPs are widely applied for the treatment of wastewater with very different composition such as industrial wastewater containing toxic compounds [14,15], sewage systems polluted with micro-pollutants [16], surface or ground water [17–19] and drinking water [20,21]. In all cases, the concentration of pollutants can be reduced from several-hundred ppm to ppb levels, which is reflected in a significant decrease Chemical Oxygen Demand (COD) and Total Organic Carbon (TOC).

It is generally accepted that the mineralization process in AOPs is the formation of CO_2 and water, and in case of nitrogen-containing pollutants, N-volatile species [22]. However, the release of toxic and hazardous components such as volatile organic compounds (VOC), volatile inorganic compounds (*e.g.* hydrogen sulphide) [23] or even CO must not be discarded. The gases produced in AOPs have been monitored in few studies. Rathi et al. [24] reported traces of SO_2, NO_2, CO_2 in the photodegradation of 50 mg/L of yellow-12 by UV/H_2O_2/Fe^{2+} at room conditions, though the quantification of these gaseous components was not provided. Later, Arena et al. [25] identified CO_2, C1 and C2 species in the gas effluent during the catalytic wet air oxidation (CWAO) of phenol at more severe operating conditions (1000 ppm of phenol, 150 °C, 1.4 MPa and 100 STP mL/min of oxygen flow rate). C1 and C2 were identified as formic and acetic acids, respectively, and represented < 5% of the off-gas. Meanwhile, CO_2 was found in higher concentrations (> 200 mg/L), values that were dependent on the typen of catalyst used [25]. Recent studies concerning the gas phase in AOP treatments have been focused on the removal of nitrogen-containing pollutants [22,26]. Garcia-Segura et al. [22] detected CO_2 and very low amounts of NO and NO_2 upon the electrochemical oxidation of 670 mg/L of 4-nitrobenzoic acid and several substituted aminobenzoic acids. Their release to the gas phase was three order of magnitude lower than the initial nitrogen in solution. In the study of Lousteau et al. [26] dealing with the CWAO of ammonia in presence of supported noble metal catalysts (200 °C, 50 bar), harmless molecular N_2 was the only species detected in the off-gas effluent. In none of these works [22–26], CO was detected in the gas phase.

The Fenton process (Fe^{2+}/Fe^{3+} + H_2O_2) is a fairly popular AOP

* Corresponding author.
E-mail address: jaime.carbajo@uam.es (J. Carbajo).

https://doi.org/10.1016/j.apcatb.2018.03.030
Received 18 January 2018; Received in revised form 2 March 2018; Accepted 9 March 2018
Available online 11 March 2018
0926-3373/

because of the operational simplicity and flexibility, easy integration into existing water remediation processes, and relative low cost in comparison to other AOPs [27]. There are currently several commercial units, *viz* PRI-TECH™, OXY-PURE®, OHP® and PeroxyChem, that demonstrate the high effectiveness of Fenton process in the treatment of many types of non-biodegradable industrial wastewater such as pharmaceutical and cosmetic, refinery and petrochemical, dyestuff, polymers, wood preservatives and plastics additives [28,29]. However, to date a detailed assessment of the gas effluent in the course of the Fenton process is still lacking.

This work, therefore, evaluates the emissions of CO_2 and CO upon the Fenton treatment of water containing phenol, a common target of AOPs studies. The influence of H_2O_2 dosage, temperature and amount of Fe^{2+} on the potential formation of CO has been evaluated. Furthermore, in order to provide a better understanding of the reaction mechanisms that are involved in the CO formation, the distribution of intermediate oxidation products in liquid phase and their respective effect on CO production has been analysed. This research is the first work dealing with the formation and emission of CO in the off-gas during Fenton oxidation process. Herein, we highlighted the importance of evaluating not only liquid phase intermediates, due to their recalcitrant and/or toxic behaviour, also the gas phase because of CO production.

2. Experimental

2.1. Chemicals

Hydrogen peroxide solution (30% w/v) and $FeCl_2{\cdot}4H_2O$ (> 98.0%) were purchased from Sigma-Aldrich. Working standard solutions of phenol, hydroquinone, resorcinol, catechol, p-benzoquinone, acetic acid, formic acid, malonic acid, maleic acid all from Sigma–Aldrich and oxalic acid (Panreac) were prepared and used for High Performance Liquid Chromatography (HPLC) and Ionic Chromatography (IC) calibration. A certified gas standard mixture (CO and CO_2 balanced in N_2) purchased from Praxair was used for quantification purposes. Other reagents used in the analyses were H_2SO_4 (Panreac), Na_2CO_3 (Panreac), $NaHCO_3$ (Merck), $TiOSO_4$ (Riedel-deHaën). HCl (37% Panreac) was used to adjust the initial pH of the reaction media. All these reagents were of analytical grade and were used without further purification. All solutions were prepared with deionized water.

2.2. Fenton experiments

Fenton runs were performed in a stainless steel high-pressure reactor (BR-300, BERGHOF) equipped with a PTFE reaction vessel of 500 mL. The reaction volume was 310 mL, and the reactants were added sequentially at the beginning of each experiment. Briefly, 300 mL of an aqueous solution containing a predefined concentration of the target pollutant and Fe^{2+} was placed in the reactor and stirred at 600 rpm. Helium (He) was used to flush the reactor while the selected temperature was achieved. Then, the appropriate volume of 30% w/v H_2O_2 solution was injected with He till reach a reactor pressure of 3 atm, this step was considered the beginning of the reaction time. Fig. 1 shows the scheme of the experimental set-up used in Fenton oxidation. The reactor operated in batch mode for both gas and liquid phases. After reaction, the gas effluent was collected in a Tedlar bag of 1 L capacity and the liquid sample was cooled and immediately analyzed.

CO yields were calculated as the amount of CO in gas phase per amount of carbon removed from the liquid phase, in mg, CO/(TOC_0-TOC).

Fenton experiments were carried out with phenol, catechol and hydroquinone and some acid mixture, consisting of acetic, formic, fumaric, malonic and maleic acids. The trails were performed at the initial concentration of 1000 mg/L of aromatics or 400 mg/L of each acid,

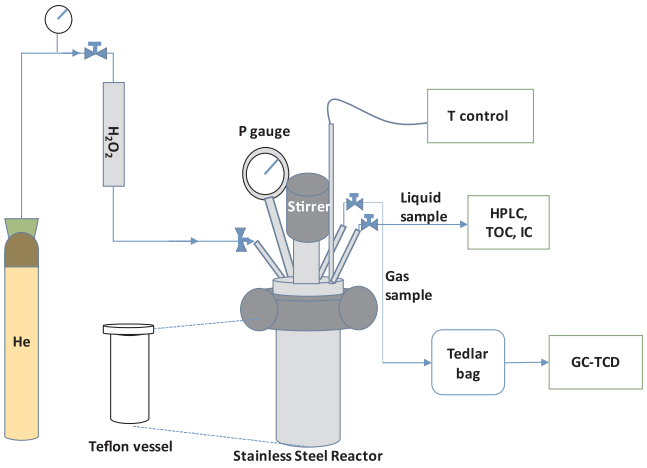

Fig. 1. Scheme of the experimental set-up of Fenton oxidation.

90 °C, 100 mg/L of Fe^{2+} and using 5000 mg/L of H_2O_2 for pollutant mineralization. The initial pH of the reaction medium was 3.

The influence of the operating conditions on the CO_2 and CO formation was studied upon phenol Fenton oxidation. The effect of the initial H_2O_2 dosage was tested within the range of 2500–15,000 mg/L, equivalent to the 50 and 300% stoichiometric requirement for phenol mineralization, respectively. The temperature and Fe^{2+} concentration were tested within 30–90 °C and 10–100 mg/L, respectively.

2.3. Analytical methods

TOC and Total Inorganic Carbon (TIC) in solution were measured using a TOC Analyzer (Shimadzu, mod. TOC-Vsch). Hydrogen peroxide concentration was analysed by colorimetric titration $TiOSO_4$ method [30] using a UV2100 Shimadzu UV–vis spectrophotometer. Aromatic compounds (*viz.* phenol, resorcinol, catechol, hydroquinone and p-benozquinone) were analysed by HPLC (Thermo Fisher Scientific) using a C18 column (Eclipse Plus C18, 150 × 4.6 mm, 5 µm) at 323 K with a 4 mM aqueous sulfuric acid solution at 1 mL/min as mobile phase. A photo-diode array detector at wavelengths of 210 and 246 nm was used. Short-chain organic acids were analysed by IC equipped with a conductivity detector (Metrohm 883 IC) using a Metrosep A supp 5 column (250 × 4 mm) as stationary phase and 0.7 mL/min of an aqueous solution of 3.2 mM Na_2CO_3 and 1 mM $NaHCO_3$ as the mobile phase.

CO_2 and CO in the Fenton gas phase were analysed in a GC (Bruker 3900 model) using a 30 m Carboxen 1000 column with He as carrier gas (30 mL/min). The GC was connected to a thermal conductivity detector (TCD) at 150 °C and the following temperature program was employed: 35 °C (5 min) to 200 °C at 20 °C /min, hold at 200 °C for 8 min.

3. Results and discussion

3.1. CO determination and carbon mass balance closure

Fig. 2 shows the evolution of phenol and short-chain organic acids (mainly oxalic and formic but also maleic, acetic and traces of malonic acid) detected upon the Fenton process at 90 °C. As it can be seen, phenol was completely converted within the first 5 min of reaction time. Due to the fast ring opening of phenol and its expected aromatic oxidation intermediates (such catechol, hydroquinone and *p*-benzoquinone, none detected), a fast TOC diminishing in the liquid occurred at the first stage of the reaction. The differences between the measured TOC values and the amount of carbon in the identified compounds (short chain acids) reveal the presence of unidentified byproducts, which are usually assigned to condensation species [31–35]. The incomplete TOC mineralization (X_{TOC} = 80% at 180 min) is related to the

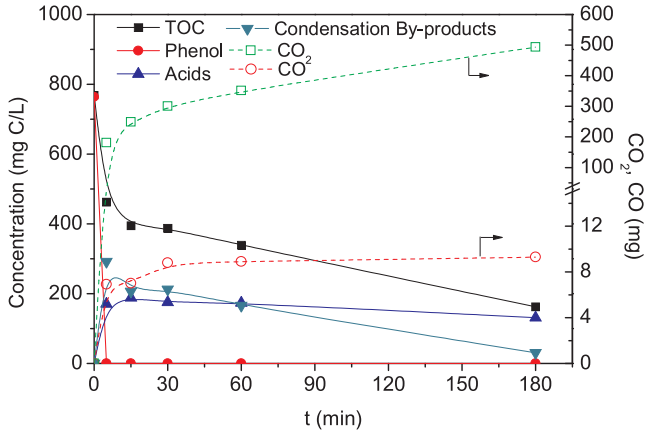

Fig. 2. Evolution of phenol, TOC and oxidation by-products on the Fenton oxidation of phenol. Operating conditions: $[Phenol]_0$ = 1000 mg/L, $[H_2O_2]_0$ = 5000 mg/L (stoich. dosage), $[Fe^{2+}]$ = 100 mg/L and T = 90 °C.

oxalic acid, partially refractory to Fenton process [35,36,37], and in less extent, to formic acid, both the unique compounds detected at the end of the reaction.

CO_2 and CO were the carbon species detected in the gaseous phase. Their evolution is also depicted in Fig. 2. Their formation mainly took place from the beginning of the reaction. Thus, 180 mg of CO_2 and 7 mg CO were quantified at 5 min of reaction. The CO_2 concentration evolved accordingly to the condensation compound disappearance reaching an amount of 493 mg after 180 min of reaction. However, CO concentration scarcely increased during the reaction progress (9 mg were produced after 180 min). This fact points out that phenol and its aromatic oxidation intermediates are the main responsible of CO production upon an incomplete mineralization.

The carbon mass balance is closed to 100% upon reaction, as is shown in Fig. 3. In this figure, the contribution of the gaseous products (*viz.* CO and CO_2) and the species in the liquid effluent (*viz.* short-chain organic acids, condensation byproducts and dissolved CO_2 quantified as TIC) is provided in terms of carbon percentage at different reaction times. The slight mismatch observed at some reaction times, always lower than 5%, might be attributed to the release of the dissolved inorganic carbon to the atmosphere during the liquid sampling from the pressurized reactor.

Attending to the CO_2 and CO production at the selected operating conditions of Fig. 3, low CO/CO_2 mass ratios were obtained and this value decreased with the reaction time, from 0.038 mg CO/mg CO_2 after 5 min of reaction to 0.019 mg/mg after 180 min. In spite of this, CO concentration in the gas phase is above 11,000 mg/Nm^3 at the final

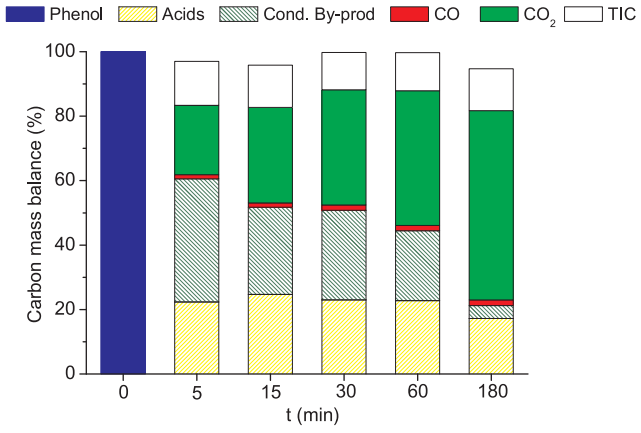

Fig. 3. Carbon distribution on the Fenton oxidation of phenol at the operating conditions of Fig. 2.

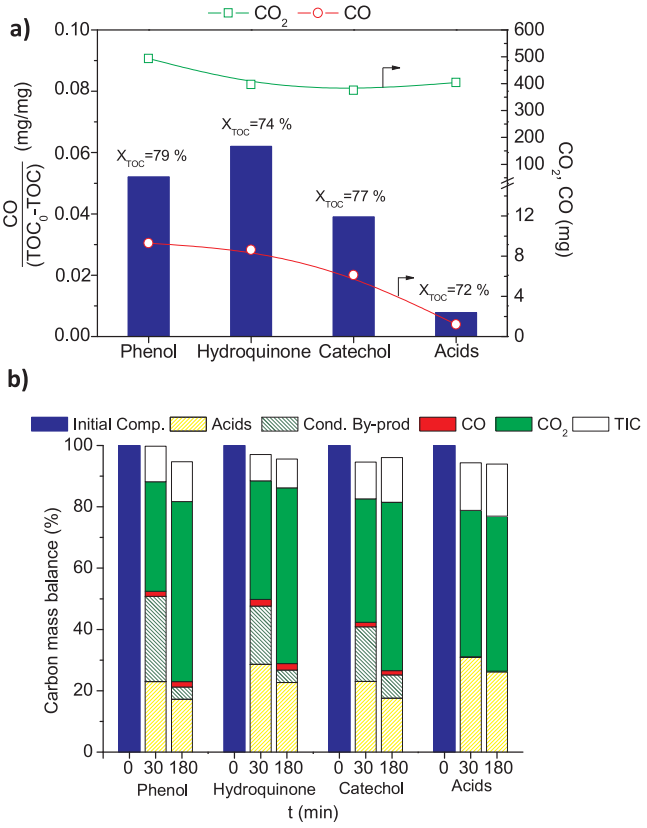

Fig. 4. Yield to CO expressed as $CO/(TOC_0\text{-}TOC)$ and total amount of CO_2 and CO in the off-gas (a) and carbon distribution (b) after 180 min reaction on the Fenton oxidation of different pollutants. $[Phenol]_0$ = $[Catechol]_0$ = $[Hidroquinone]_0$ = 1000 mg/L, a mixture of acids such as acetic, formic, fumaric, malonic and maleic: $[each\ acid]_0$ = 400 mg/L, $[H_2O_2]_0$ = 5000 mg/L, $[Fe^{2+}]$ = 100 mg/L and T = 90 °C.

reaction time, 180 min (calculations provided in the Supporting information). Considering that the emission limit value for CO according to Directive 2010/75/EU on Industrial Emissions is 100 mg/Nm^3 (as a half hourly average value) [38], CO emissions in Fenton oxidation must not be underestimated. Clearly, the gaseous effluent must be monitoring and need to be treated in gas facilities to provide Fenton as a real sustainable solution.

3.2. Effect of the organic oxidation intermediates on CO production

According to the evolution of intermediates in the Fenton oxidation of phenol (Fig. 2), the CO production can be ascribed to aromatic species (phenol and its first oxidation intermediates), which all disappeared within the first minutes of reaction. To gain an insight into the effect of the pollutant nature on the CO production, Fenton oxidation runs on different pollutants have been carried out. Hydroquinone, catechol and short-chain acids (as a mixture of acetic, formic, fumaric, malonic and maleic acids with an initial concentration of each acid in the mixture of 400 mg/L) has been studied at $[TOC]_0$ = 650–734 ppm, $[H_2O_2]_0$ = 5000 ppm, T = 90 °C and $[Fe^{2+}]_0$ = 100 ppm. The results obtained at 180 min of reaction time are shown in Fig. 4a. The phenol oxidation results obtained at the same operating conditions have been also included for the sake of comparison. As it is shown in Fig. 4a, a similar mineralization was achieved for each pollutant, X_{TOC} ~75%. However, the amount of CO produced varied with the pollutant nature. As expected, short-chain acids gave rise to the lowest CO yields, represented as $CO/(TOC_0\text{-}TOC)$, whereas this ratio was 5, 6 and 8 times higher for catechol, phenol and hydroquinone, respectively. This fact supports that the aromatic ring opening is the main step involved in the carbon monoxide production.

The differences found in the CO/(TOC_0-TOC) ratios for catechol and hydroquinone can be explained by their different oxidation routes. The double bond cleavage in hydroquinone ring to yield maleic acid, as proposed by Zazo et al. [35], seems to favour CO formation, while in catechol, the muconic acid formation before maleic acid [35] favours the mineralization to CO_2.

The carbon mass balances calculated for each initial compound upon oxidation are shown in Fig. 4b. In all cases, the sum of carbon percentage from the byproducts species in the gas and the liquid phase is closed to 100%. As it can be inferred from the reaction time evolution, in all the cases the amount of CO was produced mainly within the first 30 min of reaction time. After this period, subsequent degradation of condensation byproducts and short organic acids gave rise to CO_2 formation, confirming that the mineralization of these by-products are not predominately assigned to the release of CO.

3.3. Effect of the operating conditions on CO production

The undesired production of CO upon Fenton oxidation process could be minimized by the selection of the operating conditions. For this reason, the H_2O_2 dosage, temperature and catalyst concentration effect on the CO yield of phenol oxidation have been evaluated. The total amount of CO_2 and CO measured in the gas phase after 180 min of reaction time, along with the resulting CO/(TOC_0–TOC) ratios are shown in Fig. 5 at different operating conditions.

The CO production and CO/(TOC_0–TOC) ratios increase when the H_2O_2 dosage was varied from 50 to 200% the stoichiometric amount, and remain constant at a significant excess of H_2O_2 (from 200 to 300%), as it can be seen in Fig. 5a. At H_2O_2 dosages up to 100% the stoichiometric amount, lower CO yields are obtained while the use of H_2O_2 dosage from 100 to 200%, enhances CO formation without increasing mineralization. Note that a significant excess of H_2O_2 (from 200 to 300%) does not affect the CO yields, neither the overall oxidation efficiency nor intermediate distribution. Clearly, the excess of radical species, HO· and HOO·, promotes the autoscavenging reactions leading to an inefficient consumption of H_2O_2 [39–41].

The increasing of Fenton reaction temperature from 30 to 90 °C, Fig. 5b, leads to enhanced TOC conversion, from 35 to 81%, respectively, as has been previously reported [36]. This mineralization occurred *via* CO_2 over CO formation. In fact, the total amount of CO_2 increased by a factor of 5 whereas CO by a factor of 2, resulting in a decrease of CO/(TOC_0–TOC) with temperature. In view of these results (Fig. 5b), it is interesting to point out that the beneficial effect ascribed to high temperatures on Fenton process is not only due to the higher mineralization efficiencies [36], but also to favour CO_2 selectivity.

Lastly, the catalyst concentration effect on the CO_2 and CO production is shown in Fig. 5c. In the selected range, from 10 to 100 mg/L Fe^{2+}, TOC removal along with the total CO_2 amount increase with the catalyst load. However, the production of CO was unaffected. In all the runs, H_2O_2 was completely consumed and a higher catalyst concentration resulted in a higher efficiency. Moreover, the selectivity to CO_2 was increased while the production of CO did not sow a significant change. Therefore, CO/(TOC_0–TOC) ratio decreased as the concentration of catalyst increased.

According to the above results, H_2O_2 dosage is the most influence variable on CO production upon Fenton oxidation process. Noteworthy that the use of H_2O_2 in excess not only leads to an inefficient consumption of the oxidant but also higher CO yields. Therefore, CO emissions in Fenton processes should be considered when selecting the operating conditions, particularly in the treatment of high-loaded industrial wastewaters. Note that, in this case, the wastewater characterization is generally based on global parameters such as TOC or COD and therefore, the use of the stoichiometric H_2O_2 to organic pollutant ratio is unlike.

4. Conclusions

A gas phase with noxious concentrations of CO along with CO_2 is generated from Fenton oxidation processes. CO is mainly formed through the oxidative cleavage of aromatic rings (mainly the hydroquinone oxidation route). The CO yield of these aromatic species are from 5 to 8 times higher than that of the short-chain acids at 90 °C of reaction temperature. Also, the operating conditions such a temperature and mainly H_2O_2 dosage are crucial for the CO yields. High temperatures (> 90 °C) and stoichiometric dosage of H_2O_2 are required to assure an efficient consumption of the oxidant without improving CO yields.

Although further studies are needed, the results of this work may lead to predict the formation of CO in other AOPs than Fenton. Therefore, advanced oxidation technologies in wastewater must be conceived with a treatment strategy that integrate wastewater and gas management to assure the treatment effectiveness and sustainability expected.

Acknowledgment

Financial support from the project CTM2016-76454-R (Ministerio de Economia y Competitividad-MINECO, Spain) is gratefully acknowledged.

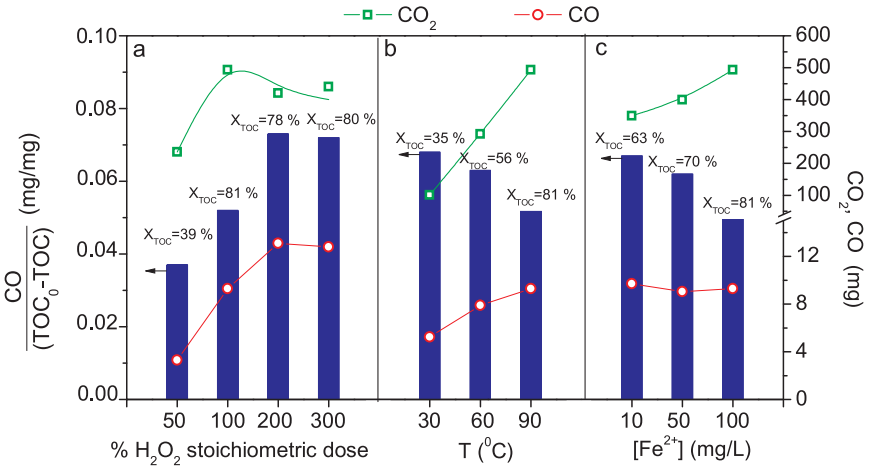

Fig. 5. Effect of H_2O_2 dosage (a), reaction temperature (b) and Fe^{2+} concentration (c) on the CO and CO_2 production upon Fenton oxidation of 1000 mg/L phenol at 180 min of reaction time.

Appendix A. Supplementary data

Supplementary material related to this article can be found, in the online version, at doi:https://doi.org/10.1016/j.apcatb.2018.03.030.

References

[1] Y. Liu, Y.G. Adewuyi, Chem. Eng. Res. Des. 112 (2016) 199–250.
[2] P. Ning, X. Wang, Front. Environ. Sci. Eng. 9 (2015) 181–189.
[3] M. Cheng, G.M. Zeng, D.L. Huang, C. Lai, P. Xu, C. Zhang, Y. Liu, Chem. Eng. J. 284 (2016) 582–598.
[4] E. Morillo, J. Villaverde, Sci. Total Environ. 586 (2017) 576–597.
[5] H. Zhang, D. Ma, R. Qiu, Y. Tang, C. Du, Chem. Eng. J. 313 (2017) 157–170.
[6] A.R. Ribeiro, O.C. Nunes, M.F.R. Pereira, A.M.T. Silva, Environ. Int. 75 (2015) 33–51.
[7] I. Oller, S. Malato, J.A. Sánchez-Pérez, Sci. Total Environ. 409 (2011) 4141–4166.
[8] J. Rivera-Utrilla, M. Sanchez-Polo, M.A. Ferro-Garcia, G. Prados-Joya, R. Ocampo-Perez, Chemosphere 93 (2013) 1268–1287.
[9] V. Homem, L. Santos, J. Environ. Manage. 92 (2011) 2304–2347.
[10] C.M.A. Oturan, J.-J. Aaron, Crit. Rev. Environ. Sci. Technol. 44 (2014) 2577–2641.
[11] M. Sillanpää, M.C. Ncibi, A. Matilainen, J. Environ. Manage. 208 (2018) 56–76.
[12] S. Garcia-Segura, E. Brillas, Appl. Catal. B: Environ. 181 (2016) 681–691.
[13] S. Garcia-Segura, E. Brillas, J. Photochem. Photobiol. C: Photochem. Rev. 31 (2017) 1–35.
[14] L. Bilinska, M. Gmurek, S. Ledakowicz, Chem. Eng. J. 306 (2016) 550–559.
[15] C.R. Holkar, A.J. Jadhav, D.V. Pinjari, N.M. Mahamuni, A.B. Pandit, J. Environ. Manage. 182 (2016) 351–366.
[16] L.L.S. Silva, J.C.S. Sales, J.C. Campos, D.M. Bila, F.V. Fonseca, Environ. Sci. Pollut. Res. 24 (2017) 6329–6338.
[17] R. Lamsal, M.E. Walsh, G.A. Gagnon, Water Res. 45 (2011) 3263–3269.
[18] G. Andreottola, L. Dallago, E. Ferrarese, J. Hazard. Mater. 156 (2008) 488–498.
[19] F.A. Caliman, B.M. Robu, C. Smaranda, V.L. Pavel, M. Gavrilescu, Clean Technol. Environ. Policy 13 (2011) 241–268.
[20] Y. Aguas, M. Hincapie, P. Fernández-Ibáñez, M.I. Polo-López, Sci. Total Environ. 607–608 (2017) 1213–1224.
[21] E.S. Massima Mouele, J.O. Tijani, O.O. Fatoba, L.F. Petrik, Environ. Sci. Pollut. Res. 22 (2015) 18345–18362.
[22] S. Garcia-Segura, E. Mostafa, H. Baltruschat, Appl. Catal. B: Environ. 207 (2017) 376–384.
[23] http://eippcb.jrc.ec.europa.eu/reference/BREF/CWW_Bref_2016_published.pdf.
[24] A. Rathi, H.K. Rajor, R.K. Sharma, J. Hazard. Mater. 102 (2003) 231–241.
[25] F. Arena, C. Italiano, A. Raneri, C. Saja, Appl. Catal. B: Environ. 99 (2010) 321–328.
[26] C. Lousteau, M. Besson, C. Descorme, Catal. Today 241 (2015) 80–85.
[27] S. Esplugas, J. Giménez, S. Contreras, E. Pascual, M. Rodríguez, Water Res. 36 (2002) 1034–1042.
[28] P. Bautista, A.F. Mohedano, J.A. Casas, J.A. Zazo, J.J. Rodriguez, J. Chem. Technol. Biotechnol. 83 (2008) 1323–1338.
[29] J.L. Wang, L.J. Xu, Crit. Rev. Environ. Sci. Technol. 42 (2012) 251–325.
[30] G. Eisenberg, Colorimetric determination of hydrogen peroxide, Ind. Eng. Chem. Anal. Ed. 15 (1943) 327–328.
[31] S. Basu, I.W. Wei, Environ. Eng. Sci. 17 (2000) 279–290.
[32] H.R. Eisenhauer, J. Water Pollut. Control Fed. 36 (1964) 1116–1128.
[33] J. Poerschmann, U. Trommler, J. Chromatogr. A 1216 (2009) 5570–5579.
[34] I. Magario, F.S. García Einschlag, E.H. Rueda, J. Zygadlo, M.L. Ferreira, J. Mol. Catal. A: Chem. 352 (2012) 1–20.
[35] J.A. Zazo, J.A. Casas, A.F. Mohedano, M.A. Gilarranz, J.J. Rodríguez, Environ. Sci. Technol. 39 (2005) 9295–9302.
[36] J.A. Zazo, G. Pliego, S. Blasco, J.A. Casas, J.J. Rodríguez, Ind. Eng. Chem. Res. 50 (2011) 866–870.
[37] S. Garcia-Segura, E. Brillas, L. Cornejo-Ponce, R. Salazar, Sol. Energy 124 (2016) 242–253.
[38] Directive 2010/75/EU on industrial emissions (Integrated Pollution prevention and control).
[39] C.C. Jiang, S.Y. Pang, F. Ouyang, J. Ma, J. Jiang, J. Hazard. Mater. 174 (2010) 813–817.
[40] J.H. Ramirez, F.J. Maldonado-Hodar, A.F. Perez-Cadenas, C. Moreno-Castilla, C.A. Costa, L.M. Madeira, Appl. Catal. B: Environ. 75 (2007) 312–332.
[41] X.F. Xue, K. Hanna, M. Abdelmoula, N.S. Deng, Appl. Catal. B: Environ. 89 (2009) 432–440.